RESEARCH ARTICLE

4D-Printing of Photoswitchable Actuators

Xili Lu,[a,b] Cedric P. Ambulo,[a] Suitu Wang,[a,d] Laura K. Rivera-Tarazona,[a,c] Hyun Kim,[a,e] Kyle Searles[a] and Taylor H. Ware*[a,c,d]

[a] Dr. X. Lu, C. P. Ambulo, S. Wang, L. K. Rivera-Tarazona, Dr. H. Kim, K. Searles, Prof. Dr. T. H. Ware
Department of Bioengineering
University of Texas at Dallas
Richardson, TX 75080, USA
[b] Current address: Dr. X. Lu
State Key Laboratory of Polymer Materials Engineering, Polymer Research Institute
Sichuan University
Chengdu 610065, China
[c] Current address: L. K. Rivera-Tarazona, Prof. Dr. T. H. Ware
Department of Biomedical Engineering
Texas A&M University
College Station, TX 77843, USA
E-mail: Taylor.Ware@tamu.edu
[d] Current address: S. Wang, Prof. Dr. T. H. Ware
Department of Materials Science and Engineering
Texas A&M University
College Station, TX 77843, USA
[e] Current address: Dr. H. Kim
Sensors and Electron Devices Directorate
CCDC Army Research Laboratory
Adelphi, MD 20783, USA

Abstract: Shape-switching behavior, where a transient stimulus induces an indefinitely stable deformation that can be recovered on exposure to another transient stimulus, is critical to building smart structures from responsive polymers as continue power is not needed to maintain deformations. Here, we 4D-print shape-switching liquid crystalline elastomers (LCEs) functionalized with supramolecular crosslinks, dynamic covalent crosslinks and azobenzene. The salient property of shape-switching LCEs is that light induces long-lived, deformation that can be recovered on-demand by heating. UV-light isomerizes azobenzene from *trans* to *cis*, and temporarily breaks the supramolecular crosslinks, resulting in a programmed deformation. After UV, the shape-switching LCEs fix more than 90% of the deformation over 3 days by the reformed supramolecular crosslinks. Using the shape-switching properties, we print Braille-like actuators that can be photoswitched to display different letters. This new class of photoswitchable actuators may impact applications such as deployable devices where continuous application of power is impractical.

Introduction

Four-dimensional (4D) printing is a manufacturing technology that originates from the integration of three-dimensional (3D) printing and stimuli-responsive materials.[1] 4D-printed structures are capable of morphing from one shape to another in response to an environmental stimulus, such as moisture,[2] magnetic field,[3] heat,[4] and light.[5] These morphing structures may enable a wide variety of intelligent devices from soft robots[3, 6] to morphing biomedical devices.[7] 4D printed objects can be designed to exhibit irreversible or reversible shape-morphing. For example, shape memory polymers (SMPs) can be printed such that a stimulus triggers an irreversible shape change.[4-5, 8] Hydrogels can be printed such that a stimulus triggers reversible shape change.[2b] In both classes of materials, the printing process itself can be used to encode the shape morphing behavior. However, neither of these strategies can be used to create shape-switching structures, where a stimulus triggers a shape change that persists indefinitely after removal of the stimulus but where the initial form can be recovered by a second stimulus without requiring mechanical intervention. The inability to induce shape switching (i.e., to "latch" a shape-changing material) is a well-known limitation in disparate classes of actuators, from the polymers described above to shape memory alloys.[9] Applications of 4D printed structures would be greatly expanded by shape-switching behavior as power is not required to maintain the deformed shape. As no class of 4D-printable materials exhibits programmable and large strain shape-switching behavior, the design of such a material will require integration of concepts from a variety of shape-changing materials.

Liquid crystal elastomers (LCEs)[10] are a class of shape-changing materials capable of large-scale, reversible deformations that make them compelling for numerous potential applications such as soft robots,[11] artificial muscles[12] and deployable devices.[13] Unlike hydrogels or SMPs, LCEs require neither aqueous environments nor external loads to undergo reversible shape change. To achieve reversible deformations in the absence of a load, mesogen alignment should be obtained prior to network crosslinking. Traditionally, mesogen alignment is obtained by mechanically stretching a gel,[14] aligning the monomer solution via interactions with surfaces,[15] or applied magnetic fields.[16] Crosslinking of the polymer network fixes the mesogen alignment, resulting in a shape-changing LCE. Recently, 4D printing has been applied to control mesogen alignment that enables 3D shape-morphing LCE architectures.[17] In these morphing LCE structures, shape varies continuously with temperature, and as such, continuous energy is needed to maintain a shape change. To address this issue, Lewis and coworkers demonstrated 3D printable and reconfigurable LCEs capable of being locked-in on demand in response to optical stimulus, allowing complex actuated states to be permanently maintained.[18] However, these LCEs lack the ability to be

repeatedly switched between locked-in and shape-changing states.

Azobenzene-functionalized LCEs (ALCEs) are photoresponsive materials where isomerization of the azobenzene moieties can be triggered to provide spatiotemporal control of shape-morphing by light.[19] These materials have been designed to undergo light-fueled shape morphing such as bending,[20] rolling,[21] walking,[22] swimming,[11a, 23] oscillating,[24] twisting,[15b, 25] and making waves.[26] These light-triggered deformations are governed by the reversible *trans-cis* photoisomerization of azobenzene and the resulting decrease of order in the LCE. However, for this type of ALCEs, only short-lived (< 24 h)[27] deformations can be achieved during the first several hours after photo-irradiation, owing to the spontaneous relaxation of *cis*-isomer of azobenzene over time. In end use implementations, the short-lived *cis*-isomer of azobenzene will limit utility or require constant/multiple energy expenditure to maintain a desired shape. Recently, fluorinated azobenzene[28] and hydrazone photoswitches[29] have been introduced into LCEs to achieve shape-switching behavior. We foresee orthogonal approaches to engineer shape-switching behavior that do not rely on changing the chromophore chemistry.

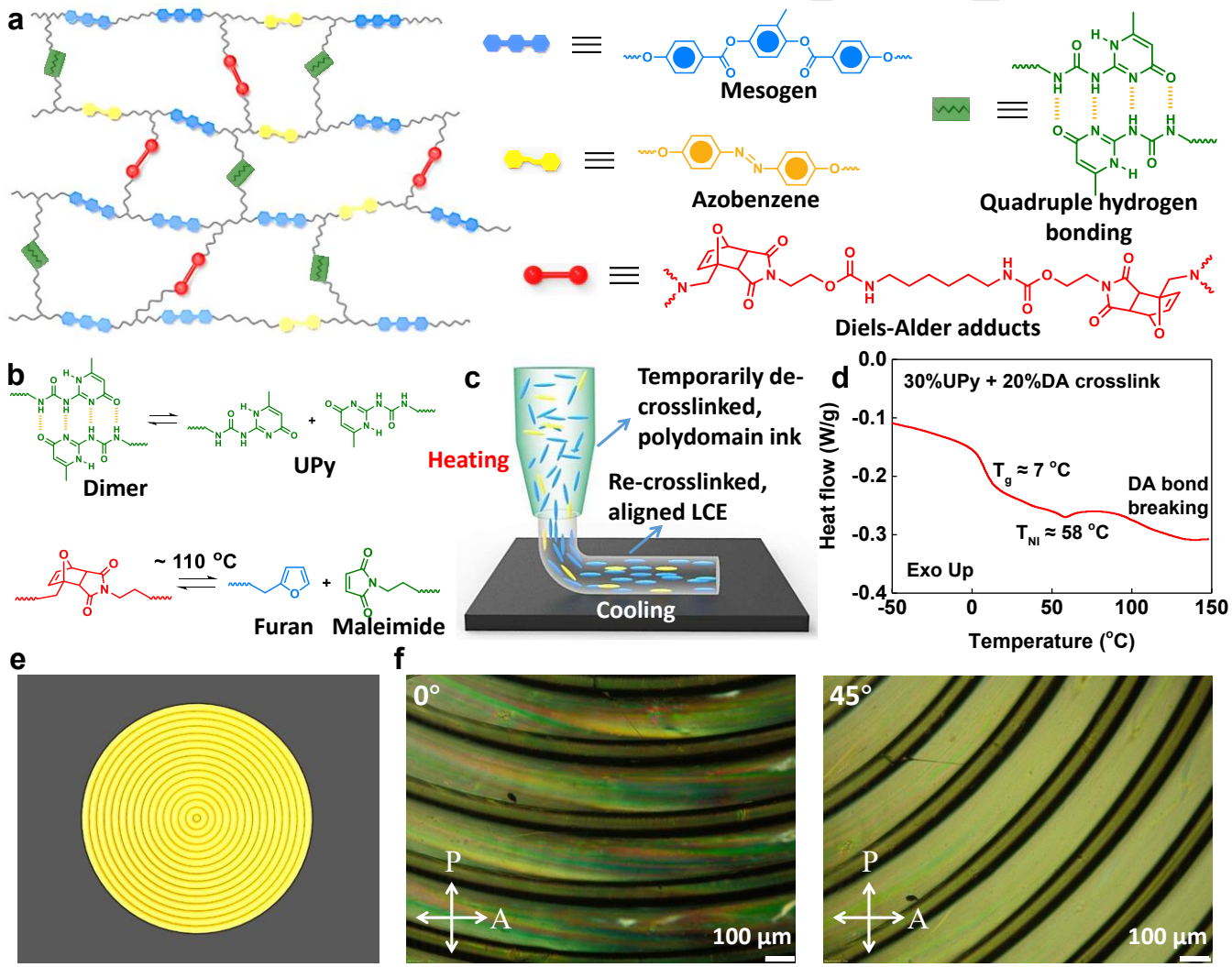

Figure 1. a) Chemical architecture of the dynamic covalent/supramolecular LCE. b) Dynamic feature of two types of reversible bonds. c) Illustration of the extrusion and programmed mesogen alignment of the SS-LCEs due to the dynamic DA bonds. d) Representative DSC trace of heating (rate of 10 °C min^{-1}) for SS-LCE_{30+20}. e) Printing path of concentric circles print pattern. f) Polarized optical micrographs showing birefringence of the printed SS-LCE_{30+20} sample when the printing direction 0° (dark) and 45° (bright) to the polarizer.

We hypothesized that LCEs could be formulated where reversible crosslinks are used to selectively decouple the shape change of the material from the isomerization of azobenzene. Specifically, 2-ureido-4[1H]-pyrimidinone (UPy)[30] has been used to fix deformation in SMPs,[31] where self-association of the UPy groups into dimers via quadruple hydrogen bonding results in physical crosslinking. UPy dimers form effective physical crosslinks due to the relatively high bonding energy (50 kJ mol^{-1}) of the dimer.[30a] During the process of light-driven actuation of ALCE, the continuous equilibrium of supramolecular interactions of UPy dimers is expected to shift to favor dissociation in response to the photothermal effect. Subsequently, the adaptive rearrangement of the supramolecular crosslinks would “lock” the shape change. This locking could prevent the spontaneous *cis*-

trans isomerization of azobenzene from inducing recovery of the material. By heating the material, these reversible crosslinks would break, and the entropic effects would drive recovery to the original state. For entropic recovery to occur, a permanent network is required during photoactuation. During printing, the material must also behave as a viscous liquid. Diels-Alder crosslinks could enable both functions if photoactuation occurs at temperatures much lower than those used during printing. With each of these functional moieties, a material could be reversibly switched from one state to another and used in either state for indefinite periods of time.

Results and Discussion

Synthesis and 3D-printing of photoswitchable LCEs

Here, we demonstrate 4D-printable ALCEs that switch reversibly and stably from one shape to another on exposure to light. The rationally designed, photoswitchable ALCEs were synthesized by introducing supramolecular interactions (UPy quadruple hydrogen bonds), reversible covalent crosslinks (furan-maleimide Diels-Alder (DA) adducts), and azobenzene into the same liquid crystal elastomer (Figure 1a). We refer to these materials as shape-switching LCEs (SS-LCEs). The general synthesis procedure for SS-LCEs is shown in Scheme S1 (Supporting Information). First, furfuryl and hydroxyl group functionalized oligomers were synthesized through aza-Michael addition[15a] between diacrylate LC mesogens (RM82 and azobenzene) and amines (furfurylamine and 5-amino-1-pentanol) at a stoichiometric mole ratio (1:1). In this study, the mole ratio of RM82 over azobenzene was maintained at 9:1 for all samples, and the amine mole ratio (furfurylamine/5-amino-1-pentanol) varied to afford the oligomers with different amount of furfuryl and hydroxyl groups. Then, the SS-LCEs were obtained by functionalization with UPy via a hydroxyl-isocyanate reaction and then crosslinking with a bismaleimide monomer (Scheme S1, Figure S1-S8, Supporting Information) via the DA reaction. The final products with different amount of UPy groups and DA crosslinks are referred as SS-LCE$_{x+y}$ where x and y represent the content of UPy groups and DA crosslinks respectively (for example, SS-LCE$_{30+20}$ means that the content of UPy groups and DA crosslinks is 30% and 20% respectively, see the Supporting Information for detailed synthesis and samples preparation, Scheme S1, Supporting Information).

DA crosslinks enable direct ink write printing of SS-LCEs. Unlike other exchangeable bonds[14b, 32] incorporated in LCEs, the furan-maleimide DA adduct is fully decoupled at relatively lower temperatures (>110 °C).[33] This approach is motivated by previous work showing that incorporating DA bonds into LCEs enables easily programmable and processable actuators.[34] During printing, the materials were heated up to 130 °C and maintained at this temperature for about 10 min to allow retro-DA reactions and temporary de-crosslinking of the polymer network (Figure 1b,c). The resulting linear LCEs can be extruded during direct ink writing. As has been previously reported,[17] the liquid crystal phase orients along the print direction (Figure 1c). Upon heating, the SS-LCE$_{30+20}$ displays a glass transition temperature (T_g) at 7 °C, a nematic-isotropic phase transition (T_{NI}) at 58 °C and DA decoupling (T_{DA}) above 110 °C, as measured by differential scanning calorimetry (DSC) (Figure 1d, Figure S9, Supporting Information). Dynamic mechanical analysis supports the identification of these transitions. Additionally, another broad transition can be observed near 55 °C (Figure S10, Supporting Information), which corresponds to the dissociation temperature of the UPy dimers.[31] Upon cooling, the decoupled furan and maleimide moieties form cycloaddition adducts and the UPy groups associate, enabling the fixation of alignment, re-crosslinking of the polymer network, and chemical welding between printing filaments. To demonstrate the fixation of programmed mesogen alignment by reversible DA bonds, we first printed single-layer, concentric circles with a diameter of 1 mm and a thickness of 0.25 mm (Figure 1e). The polarized optical micrographs of the printed concentric circles show that the printed SS-LCE film is dark when the direction of extrusion (i.e., direction of molecular alignment) is parallel to the polarizer or analyzer, and the film is bright when the extrusion direction is 45° to the polarizer (Figure 1f), indicating the mesogen alignment is retained after printing.

The effect of UPy on shape-switching behavior

To elucidate the effect of supramolecular interactions on shape switching behavior of SS-LCEs, we first printed “flower-like” actuators with alignment along the long axis of each petal. The resulting structure is approximately 5 uniaxially aligned cantilevers joined together. The composition of the SS-LCEs was varied with different amounts of UPy groups and DA bonds. Similarly to previously reported ALCEs,[20] the printed SS-LCE actuators undergo photocontrolled, reversible bending and unbending deformation in response to UV (unless otherwise stated, 365 nm UV light of 480 mW cm^{-2} intensity) and visible light (450 nm, 110 mW cm^{-2}) respectively (Figure 2a,b). It is known that upon exposure to UV light, most incident photons (up to 99%) are absorbed within the surface layer due to the high extinction coefficient of azobenzene moieties (about 2.0 × 10^4 L mol^{-1} cm^{-1} at 365 nm).[35] Therefore, the *trans*-*cis* photoisomerization of the azobenzene and the associated decrease in mesogen alignment should take place primarily in the actuator surface region. As a result, an uneven distribution of the anisotropic deformation is formed, and bending is observed in the printed SS-LCEs.

Critically, it is found that the bending deformation of SS-LCEs can be maintained at ambient conditions over timescales much longer than the relaxation of the *cis*-isomer when UPy crosslinks are present (Figure 2a,b). Under irradiation with UV light, the photothermal effect heats the illuminated region above the UPy dissociation temperature (Figure S11, Supporting Information). On removal of the light, the *cis*-isomer persists for hours, but the UPy crosslinks reform immediately as the sample passively cools. As a result, the photothermal effect enables the adaptive rearrangement/reorganization of the supramolecular polymer network to “lock” the shape change.

The effect of UPy on the shape persistence of the SS-LCE can be quantified by monitoring the relaxation of the deformed state after irradiation with UV light. Figure 2c compares the normalized height (Figure S12, see Supporting Information for definition), as measured by the tip displacement of each petal after irradiation is complete and the sample has returned to room temperature, of actuators with different concentrations of UPy (SS-LCE$_{60+20}$, SS-LCE$_{30+20}$ and SS-LCE$_{0+20}$) over a period of 72 h. The deformation of SS-LCE$_{60+20}$ and SS-LCE$_{30+20}$ is largely retained (around 95±3% and 90±11% respectively) over 72 h, while the

deformation of SS-LCE$_{0+20}$ experiences a dramatic decrease by fixing only 23±2% of the shape change after 12 h. This very limited shape fixing behavior is consistent with the behavior of other ALCEs with low crosslink density.[19] The recovery of the initial state in the dark has previously been associated with the spontaneous *cis-trans* isomerization over hours at room temperature and is the expected behavior of ALCEs based on numerous reports in the literature.[36] The stark contrast between samples with and without UPy demonstrates that the UPy supramolecular interactions are critical to long-term shape persistence after irradiation. By heating the UPy containing samples at 65 °C for 5 min, the original shape can be recovered as the UPy crosslinks dissociate, and the polymer network undergoes entropic recovery as dictated by the DA network. This heating completes a single shape switching cycle, where the actuator remains in one of two preprogrammed shapes for indefinite time periods in the absence of applied power.

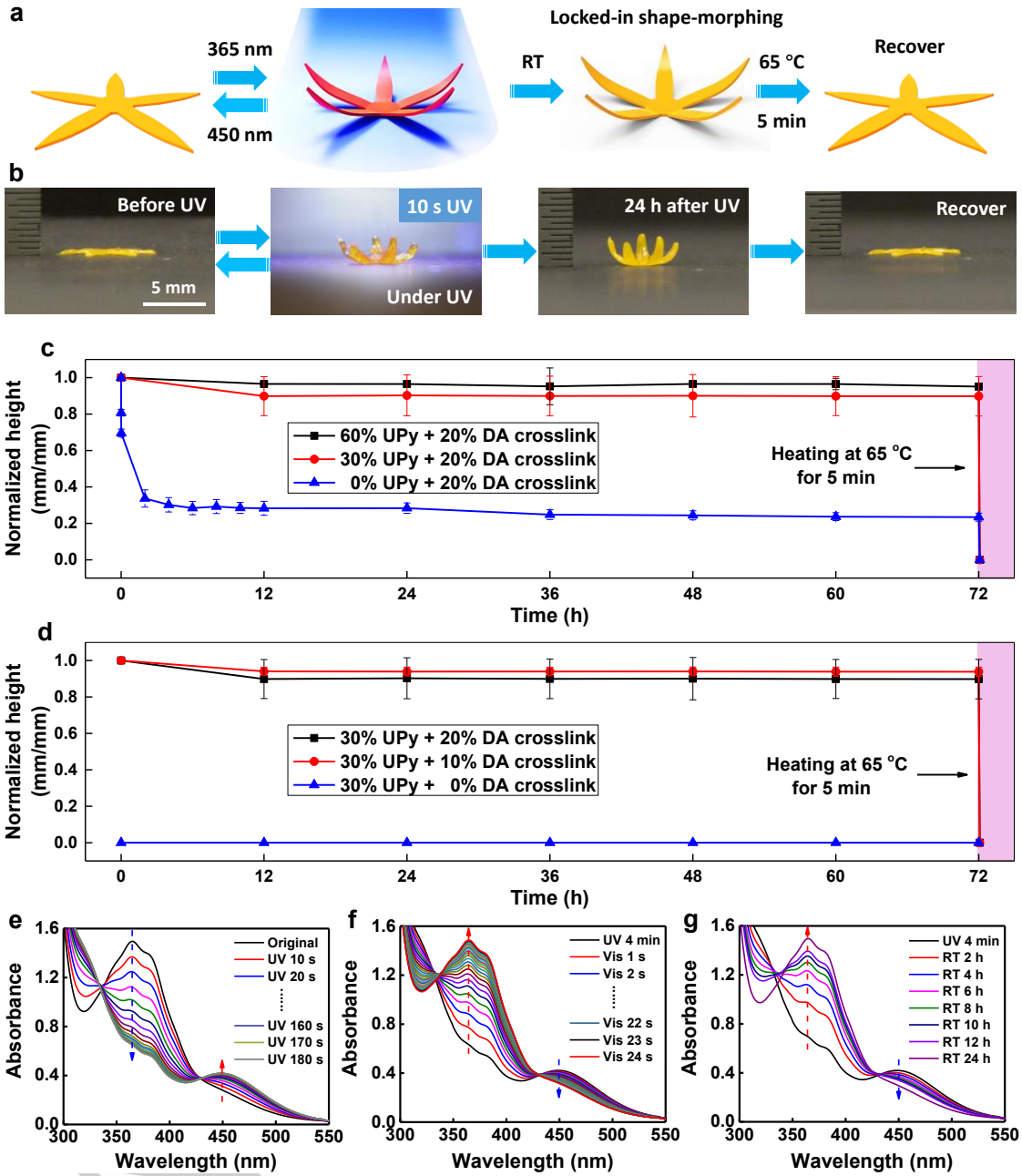

Figure 2. a) Illustration and b) photographs showing photoswitchable deformations of a flower-like actuator printed with SS-LCE$_{30+20}$. Representative curve of normalized height as a function of time of the printed SS-LCEs with different amount of c) UPy groups and d) DA crosslinks. All data represent an average value of 15 measurements from three samples, and all error bars are standard deviations. e) Changes in the absorption spectra of a stretch-aligned SS-LCE$_{30+20}$ monodomain thin film (10 µm thick, 100% strain) upon irradiation with UV light (365 nm, 4 mW cm^{-2}) for different periods of time. Changes in the absorption spectra of the UV-preilluminated (365 nm, 4 mW cm^{-2}, 4 min) SS-LCE$_{30+20}$ film (film of Figure 2e) f) upon exposure to visible light (450 nm, 10 mW cm^{-2}) and g) during spontaneous *cis-trans* relaxation of azobenzene mesogens for different periods of time.

The effect of DA crosslinks on shape-switching behavior

The covalent crosslinking of the network is also important to the shape switching behavior. The effect of DA bond content on the deformation locking was investigated by varying the DA bond amount of SS-LCE with a constant UPy concentration of 30% (SS-LCE$_{30+20}$, SS-LCE$_{30+10}$ and SS-LCE$_{30+0}$, Figure 2d). Upon exposure to UV light, actuators of all three compositions bend towards the UV light. The printed SS-LCE$_{30+0}$ actuator only transiently bends during the first 7 s then relaxes and flows (Movie S1, Supporting Information), as there are no covalent crosslinks. By contrast, the deformation of SS-LCE$_{30+20}$ and SS-LCE$_{30+10}$ is largely retained (90±11% and 94±3%, respectively). However, the amplitude of the bending of the LCE$_{30+10}$ is smaller than that of SS-LCE$_{30+20}$ (Figure S13, Supporting Information). We expect that this smaller deformation may arise from relatively poor alignment fixation after printing when the DA concentration is low. To further elucidate the role of alignment on shape-switching, the mesogen alignment of an SS-LCE$_{30+20}$ actuator was erased by heating at 130 °C for 1 min, resulting in a polydomain sample. This polydomain actuator does not undergo noticeable bending in response to UV light (Figure S14, Supporting Information). Although thin polydomain ALCEs bend in response to linearly polarized light,[20, 37] the magnitude of deformation is low as compared to oriented ALCEs, which likely explains why no obvious bending is observed in these relatively thick, unaligned actuators.

Photochemistry of shape-switching behavior

The mechanism of shape-switching can be further supported by spectroscopic measurements. UV–vis spectra were collected on a stretch-aligned SS-LCE$_{30+20}$ monodomain thin film (10 μm thick, 100% strain); a thin film was used to maximize the intensity of transmitted light. Under UV light (365 nm, 4 mW cm^{-2}) irradiation for different periods of time between 10 s and 180 s, the absorption band in the 430-500 nm region (absorption of *cis*-isomer of azobenzene) of the SS-LCE$_{30+20}$ film increases due to the *trans-cis* photoisomerization of the azobenzene moieties (Figure 2e). Subsequently, upon exposure to visible light (450 nm, 10 mW cm^{-2}), the absorption band gradually decreases to the initial value after 24 s (Figure 2f), indicating the *cis-trans* reverse-isomerization. This behavior has been reported in a wide range of azobenzene-containing polymers.[36] As expected, even without visible light irradiation, the absorption band (430-500 nm) of *cis*-azobenzene can gradually decrease to the original value after 24 h due to the spontaneous *cis-trans* reverse-isomerization (Figure 2g). This return to the globally-stable *trans*-isomer confirms that the photochemical behavior of the chromophore is not dramatically altered from previous reports.[36] It is likely that this process introduces the small decrease of the fixed deformation of SS-LCEs over the initial 12 h (Figure 2c,d). We emphasize that, despite this *cis-trans* isomerization, the deformation of SS-LCEs with UPy crosslinks is largely retained long after the completion of the *cis-trans* reverse-isomerization of azobenzene. Effectively, the supramolecular crosslinks can selectively decouple the shape change of the material from the isomerization of azobenzene.

Characterization of repeated shape-switching actuations

The shape-switching behavior of these LCEs is stable over repeated cycling, despite the lack of a permanent covalent network. Shape-switching stability of the material was probed by repeatedly irradiating the printed SS-LCE$_{30+20}$ with UV light. Since the spontaneous *cis-trans* isomerization of the *cis*-azobenzene is nearly complete within 12 h, as shown in Figure 2g, the sample was stored for 24 h in the dark during each cycle to provide enough time for relaxation of *cis*-azobenzene. The deformation in the sample was measured 60 s after UV irradiation to allow the sample to return to room temperature, 24 h after irradiation, and after heating to 65 °C for 5 min then cooling to room temperature. The results show that most of the shape change (varying from 93 ±11% to 95±12%) is maintained during the ten cycles of shape-switching experiments (Figure 3a). The polarized UV–vis spectra of a stretch-aligned SS-LCE$_{30+20}$ monodomain thin film was recorded to detect any change in order parameter (Figure 3b), which would indicate a change in alignment, after multiple cycles of UV and visible light irradiation. In each cycle, the sample was exposed to one light treatment of first UV (365 nm, 4 mW cm^{-2}, 4 min) and then visible (450 nm, 10 mW cm^{-2}, 30 s) light irradiation. Based on the polarized UV−vis spectra, the order parameter of the monodomain film is calculated to be 0.39 after processing, 0.36 after one “UV+Vis” cycle, and 0.31 after ten “UV+Vis” cycles (Supporting Information). This measurement confirms that about 80% of the azobenzene alignment is maintained even after ten cycles of UV and visible light irradiation.

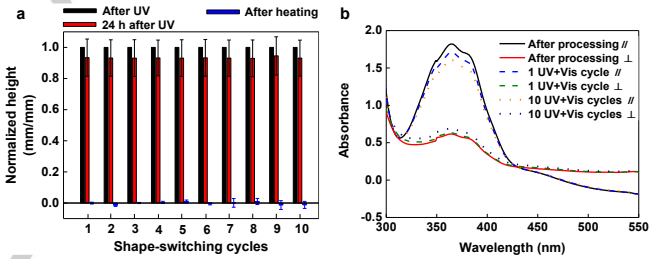

Figure 3. a) Representative curve of normalized bending height as a function of shape-switching cycles. All data are collected from the average value of three samples and all errors are standard deviations. b) Polarized absorption spectra (both parallel and perpendicular to the alignment) of a stretch-aligned SS-LCE$_{30+20}$ monodomain thin film (10 μm thick, 100% strain) after processing and after exposure to UV light (365 nm, 4 mW cm^{-2}, 4 min) and then visible light (450 nm, 10 mW cm^{-2}, 30 s) once and after ten UV+Vis exposures.

Braille-like actuator

Finally, we demonstrated a proof-of-concept application by printing a Braille-like actuator using SS-LCE$_{30+20}$, which can be switched to display different letters. LCEs have been proposed for haptic and Braille displays due to their reconfigurable shape.[38] However, continuous thermal power or periodic optical power would be required to maintain the deformed state using previously reported LCEs. Generally, a full Braille cell includes six raised dots arranged in two columns, which can be used to represent a letter, digit, punctuation mark, or word. Similarly, the printed Braille-like actuator is a rectangular substrate and six printed Archimedean chord patterns (diameter 6 mm), where the mesogen orientation varies azimuthally around a point (Figure 4a). Each Archimedean chord pattern morphs into a cone on exposure to UV light, as would be expected based on predictions[39] and

experiments in surface-aligned liquid crystal polymer networks.[40] We note that cone forms with the apex pointing away from the incident light (Figure 4b). By spatially-patterning the UV light exposure, our Braille-like actuator can be programmed to read "L", "C" and "E", by switching the shape-morphing of the Archimedean chord patterns with UV light and heating (Figure 4c, Figure S15, Supporting Information). The shape-switching feature of the Braille-like actuator can be observed using topographical images, which show that most of the deformation is retained after UV light irradiation for 24 h and can be recovered by heating (Figure 4d).

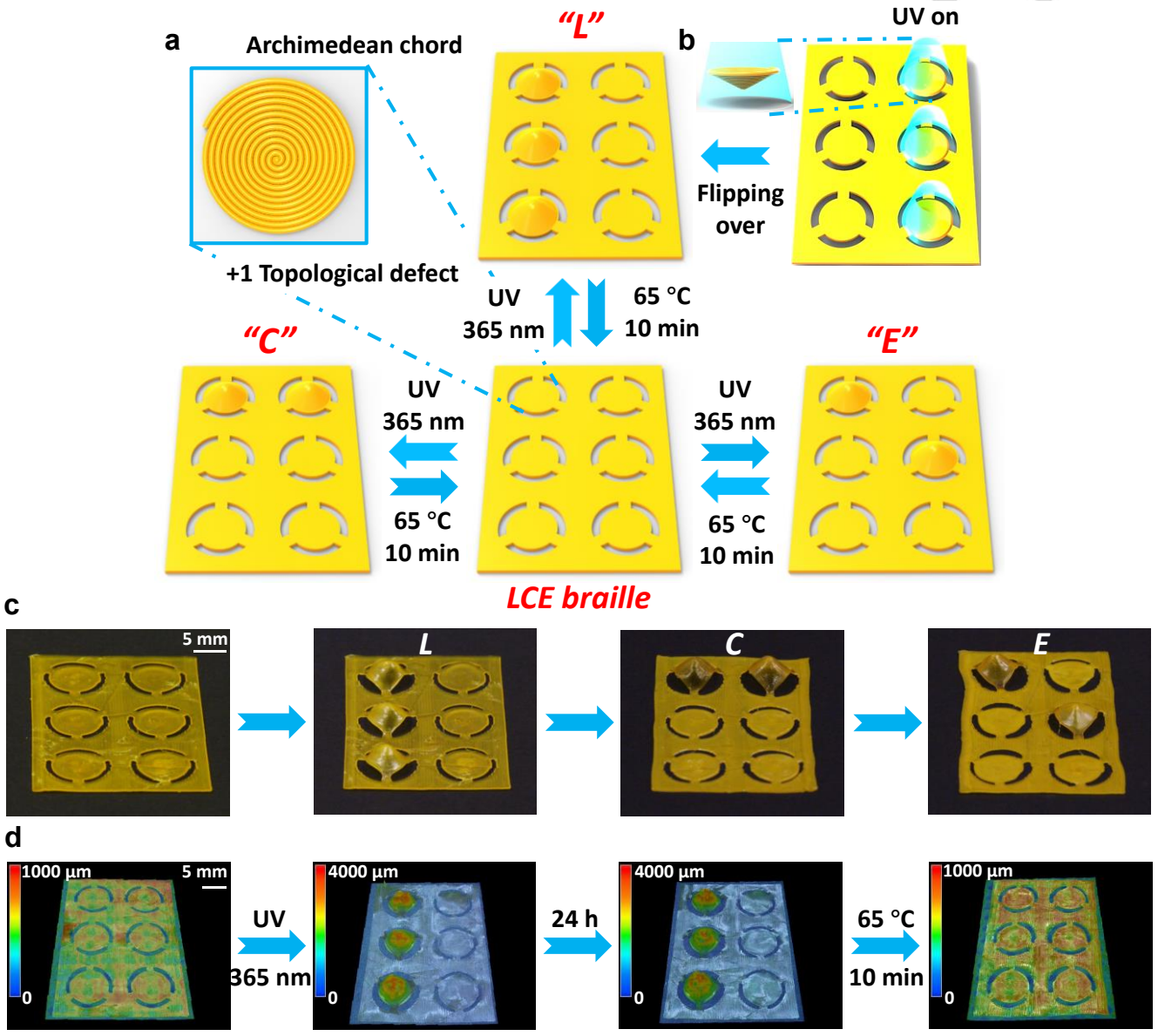

Figure 4. a) Illustration showing photoswitchable deformations of a Braille-like actuator. b) Illustration showing the photodeformation-process of a Braille-like actuator: from "flat" to "L" shape. c) Photographs showing a Braille-like actuator printed with SS-LCE$_{30+20}$ capable of displaying letters "L", "C" and "E" by switching the shape-morphing of the Archimedian chord patterns with UV light and heating. Images show actuator form 24 h after UV exposure. d) Micrographs recording the topography of the actuator during one cycle of shape switching of the Braille-like actuator between the "flat" and "L" shapes.

Conclusion

In summary, we have synthesized 4D printable, LCEs via the integration of UPy supramolecular interactions, dynamic DA crosslinks, and azobenzene within the same liquid crystal elastomer. This programmable and complex shape change of these materials is stable after irradiation with UV light. This stability arises from a decoupling of the isomerization. The original printed form can then be recovered on demand by heating. We elucidate the competitive relationship between the supramolecular interactions and covalent network on shape-switching behavior. Moreover, multiple shape-switching deformations are demonstrated by applying ten-cycle deformation locking and recover. We anticipate that this new class of photoswitchable actuators could find utility in end-use

applications such as deployable medical devices and morphing architectures.

Acknowledgements

This material is partially based upon work supported by the National Science Foundation under Grant No. 1752846 and from the Air Force Office of Scientific Research under award number FA9550-17-1-0328.

Keywords: liquid crystal elastomers • 4D printing • shape switching • azobenzene • photoswitchable actuators

[1] S. Tibbits, *Architectural Design* **2014**, 84, 116-121.

[2] a) D. Raviv, W. Zhao, C. McKnelly, A. Papadopoulou, A. Kadambi, B. Shi, S. Hirsch, D. Dikovsky, M. Zyracki, C. Olguin, R. Raskar, S. Tibbits, *Sci. Rep.* **2014**, 4, 7422; b) A. Sydney Gladman, E. A. Matsumoto, R. G. Nuzzo, L. Mahadevan, J. A. Lewis, *Nat. Mater.* **2016**, 15, 413-418.

[3] Y. Kim, H. Yuk, R. Zhao, S. A. Chester, X. Zhao, *Nature* **2018**, 558, 274-279.

[4] Z. Ding, C. Yuan, X. Peng, T. Wang, H. J. Qi, M. L. Dunn, *Sci. Adv.* **2017**, 3, e1602890.

[5] H. Yang, W. R. Leow, T. Wang, J. Wang, J. Yu, K. He, D. Qi, C. Wan, X. Chen, *Adv. Mater.* **2017**, 29, 1701627.

[6] a) S. Felton, M. Tolley, E. Demaine, D. Rus, R. Wood, *Science* **2014**, 345, 644-646; b) M. Wehner, R. L. Truby, D. J. Fitzgerald, B. Mosadegh, G. M. Whitesides, J. A. Lewis, R. J. Wood, *Nature* **2016**, 536, 451-455.

[7] a) G. Villar, A. D. Graham, H. Bayley, *Science* **2013**, 340, 48-52; b) R. J. Morrison, S. J. Hollister, M. F. Niedner, M. G. Mahani, A. H. Park, D. K. Mehta, R. G. Ohye, G. E. Green, *Sci. Transl. Med.* **2015**, 7, 285ra64.

[8] M. Zarek, M. Layani, I. Cooperstein, E. Sachyani, D. Cohn, S. Magdassi, *Adv. Mater.* **2016**, 28, 4449-4554.

[9] Y. Haga, W. Makishi, K. Iwami, K. Totsu, K. Nakamura, M. Esashi, *Sens. Actuators, A* **2005**, 119, 316-322.

[10] a) C. Ohm, M. Brehmer, R. Zentel, *Adv. Mater.* **2010**, 22, 3366-3387; b) T. J. White, D. J. Broer, *Nat. Mater.* **2015**, 14, 1087-1098.

[11] a) S. Palagi, A. G. Mark, S. Y. Reigh, K. Melde, T. Qiu, H. Zeng, C. Parmeggiani, D. Martella, A. Sanchez-Castillo, N. Kapernaum, F. Giesselmann, D. S. Wiersma, E. Lauga, P. Fischer, *Nat. Mater.* **2016**, 15, 647-653; b) H. Zeng, P. Wasylczyk, D. S. Wiersma, A. Priimagi, *Adv. Mater.* **2018**, 30, 1703554.

[12] a) H. Wermter, H. Finkelmann, *e-polym.* **2001**, 1, 013; b) D. L. Thomsen, P. Keller, J. Naciri, R. Pink, H. Jeon, D. Shenoy, B. R. Ratna, *Macromolecules* **2001**, 34, 5868-5875.

[13] H. Aharoni, Y. Xia, X. Zhang, R. D. Kamien, S. Yang, *PNAS* **2018**, 115, 7206-7211.

[14] a) M. Camacho-Lopez, H. Finkelmann, P. Palffy-Muhoray, M. Shelley, *Nat. Mater.* **2004**, 3, 307-310; b) Z. Pei, Y. Yang, Q. Chen, E. M. Terentjev, Y. Wei, Y. Ji, *Nat. Mater.* **2014**, 13, 36-41.

[15] a) T. H. Ware, M. E. McConney, J. J. Wie, V. P. Tondiglia, T. J. White, *Science* **2015**, 347, 982-984; b) S. Iamsaard, S. J. Aßhoff, B. Matt, T. Kudernac, J. L. M. CornelissenJeroen, S. P. Fletcher, N. Katsonis, *Nat. Chem.* **2014**, 6, 229-235.

[16] a) M.-H. Li, P. Keller, J. Yang, P.-A. Albouy, *Adv. Mater.* **2004**, 16, 1922-1925; b) H. Yang, A. Buguin, J.-M. Taulemesse, K. Kaneko, S. Méry, A. Bergeret, P. Keller, *J. Am. Chem. Soc.* **2009**, 131, 15000-15004; c) Y. Yao, J. T. Waters, A. V. Shneidman, J. Cui, X. Wang, N. K. Mandsberg, S. Li, A. C. Balazs, J. Aizenberg, *PNAS* **2018**, 115, 12950-12955; d) J. T. Waters, S. Li, Y. Yao, M. M. Lerch, M. Aizenberg, J. Aizenberg, A. C. Balazs, *Sci. Adv.* **2020**, 6, eaay5349.

[17] a) C. P. Ambulo, J. J. Burroughs, J. M. Boothby, H. Kim, M. R. Shankar, T. H. Ware, *ACS Appl. Mater. Interfaces* **2017**, 9, 37332-37339; b) M. López-Valdeolivas, D. Liu, D. J. Broer, C. Sánchez-Somolinos, *Macromol. Rapid Commun.* **2018**, 39, 1700710; c) A. Kotikian, R. L. Truby, J. W. Boley, T. J. White, J. A. Lewis, *Adv. Mater.* **2018**, 30, 1706164.

[18] E. C. Davidson, A. Kotikian, S. Li, J. Aizenberg, J. A. Lewis, *Adv. Mater.* **2020**, 32, 1905682.

[19] S.-k. Ahn, T. H. Ware, K. M. Lee, V. P. Tondiglia, T. J. White, *Adv. Funct. Mater.* **2016**, 26, 5819-5826.

[20] Y. Yu, M. Nakano, T. Ikeda, *Nature* **2003**, 425, 145.

[21] a) M. Yamada, M. Kondo, J.-i. Mamiya, Y. Yu, M. Kinoshita, C. J. Barrett, T. Ikeda, *Angew. Chem.* **2008**, 120, 5064–5066; *Angew. Chem. Int. Ed.* **2008**, 47, 4986-4988; b) X. Lu, S. Guo, X. Tong, H. Xia, Y. Zhao, *Adv. Mater.* **2017**, 29, 1606467; c) J. J. Wie, M. R. Shankar, T. J. White, *Nat. Commun.* **2016**, 7, 13260.

[22] a) Y. Liu, B. Xu, S. Sun, J. Wei, L. Wu, Y. Yu, *Adv. Mater.* **2017**, 29, 1604792; b) X. Lu, H. Zhang, G. Fei, B. Yu, X. Tong, H. Xia, Y. Zhao, *Adv. Mater.* **2018**, 30, 1706597.

[23] H. Shahsavan, A. Aghakhani, H. Zeng, Y. Guo, Z. S. Davidson, A. Priimagi, M. Sitti, *PANS* **2020**, 117, 5125-5133.

[24] a) K. Kumar, C. Knie, D. Bléger, M. A. Peletier, H. Friedrich, S. Hecht, D. J. Broer, M. G. Debije, A. P. H. J. Schenning, *Nat. Commun.* **2016**, 7, 11975; b) A. H. Gelebart, G. Vantomme, E. W. Meijer, D. J. Broer, *Adv. Mater.* **2017**, 29, 1606712; c) H. Zeng, M. Lahikainen, L. Liu, Z. Ahmed, O. M. Wani, M. Wang, H. Yang, A. Priimagi, *Nat. Commun.* **2019**, 10, 5057.

[25] S. J. Aßhoff, F. Lancia, S. Iamsaard, B. Matt, T. Kudernac, S. P. Fletcher, N. Katsonis, *Angew. Chem.* **2017**, 129, 3309-3313; *Angew. Chem. Int. Ed.* **2017**, 56, 3261-3265.

[26] A. H. Gelebart, D. Jan Mulder, M. Varga, A. Konya, G. Vantomme, E. W. Meijer, R. L. B. Selinger, D. J. Broer, *Nature* **2017**, 546, 632-636.

[27] a) T. Ikeda, J.-i. Mamiya, Y. Yu, *Angew. Chem.* **2017**, 129, 3309-3313; *Angew. Chem. Int. Ed.* **2007**, 46, 506-528; b) C. Barrett, A. Natansohn, P. Rochon, *Chem. Mater.* **1995**, 7, 899-903.

[28] a) S. Iamsaard, E. Anger, S. J. Aßhoff, A. Depauw, S. P. Fletcher, N. Katsonis, *Angew. Chem.* **2016**, 128, 10062-10066; *Angew. Chem. Int. Ed.* **2016**, 55, 9908-9912; b) B. R. Donovan, V. M. Matavulj, S.-k. Ahn, T. Guin, T. J. White, *Adv. Mater.* **2019**, 31, 1805750.

[29] A. Ryabchun, Q. Li, F. Lancia, I. Aprahamian, N. Katsonis, *J. Am. Chem. Soc.* **2019**, 141, 1196-1200.

[30] a) S. H. M. Söntjens, R. P. Sijbesma, M. H. P. van Genderen, E. W. Meijer, *J. Am. Chem. Soc.* **2000**, 122, 7487-7493; b) B. J. B. Folmer, R. P. Sijbesma, R. M. Versteegen, J. A. J. van der Rijt, E. W. Meijer, *Adv. Mater.* **2000**, 12, 874-878.

[31] a) J. Li, J. A. Viveros, M. H. Wrue, M. Anthamatten, *Adv. Mater.* **2007**, 19, 2851-2855; b) T. Ware, K. Hearon, A. Lonnecker, K. L. Wooley, D. J. Maitland, W. Voit, *Macromolecules* **2012**, 45, 1062-1069; c) G. Zhang, Q. Zhao, W. Zou, Y. Luo, T. Xie, *Adv. Funct. Mater.* **2016**, 26, 931-937.

[32] a) Y. Wu, Y. Yang, X. Qian, Q. Chen, Y. Wei, Y. Ji, *Angew. Chem.* **2020**, 132, 4808-4814; *Angew. Chem. Int. Ed.* **2020**, 59, 4778-4784; b) M. O. Saed, A. Gablier, E. M. Terentejv, *Adv. Funct. Mater.* **2020**, 30, 1906458; c) M. O. Saed, E. M. Terentjev, *ACS Macro Letters* **2020**, 9, 749-755.

[33] A. Gandini, *Prog. Polym. Sci.* **2013**, 38, 1-29.

[34] Z. Jiang, Y. Xiao, L. Yin, L. Han, Y. Zhao, *Angew. Chem.* **2020**, 132, 4955-4961; *Angew. Chem. Int. Ed.* **2020**, 132, 4955-4961.

[35] a) T. Yoshino, M. Kondo, J.-i. Mamiya, M. Kinoshita, Y. Yu, T. Ikeda, *Adv. Mater.* **2010**, 22, 1361-1363; b) M. Kondo, Y. Yu, T. Ikeda, *Angew. Chem.* **2006**, 118, 1406-1410; *Angew. Chem. Int. Ed.* **2006**, 45, 1378-1382.

[36] a) H. Yu, T. Ikeda, *Adv. Mater.* **2011**, 23, 2149-2180; b) T. Ube, T. Ikeda, *Angew. Chem.* **2014**, 126, 10456-10465; *Angew. Chem. Int. Ed.* **2014**, 53, 10290-10299.

[37] L. Cheng, Y. Torres, K. M. Lee, A. J. McClung, J. Baur, T. J. White, W. S. Oates, *J. Appl. Phys.* **2012**, 112, 013513.

[38] a) N. Torras, K. E. Zinoviev, C. J. Camargo, E. M. Campo, H. Campanella, J. Esteve, J. E. Marshall, E. M. Terentjev, M. Omastová, I. Krupa, P. Teplický, B. Mamojka, P. Bruns, B. Roeder, M. Vallribera, R. Malet, S. Zuffanelli, V. Soler, J. Roig, N. Walker, D. Wenn, F. Vossen, F. M. H. Crompvoets, *Sens. Actuators, A* **2014**, 208, 104-112; b) C. J. Camargo, H. Campanella, J. E. Marshall, N. Torras, K. Zinoviev, E. M. Terentjev, J. Esteve, *J. Micromech. Microeng.* 2**012**, 22, 075009.

[39] C. D. Modes, K. Bhattacharya, M. Warner, Proc. R. Soc. A 2011, 467, 1121-1140.

[40] L. T. de Haan, C. Sánchez-Somolinos, C. M. W. Bastiaansen, A. P. H. J. Schenning, D. J. Broer, *Angew. Chem.* **2012**, 124, 12637-12640; *Angew. Chem. Int. Ed.* **2012**, 51, 12469-12472.

4D-Printing of Photoswitchable Actuators

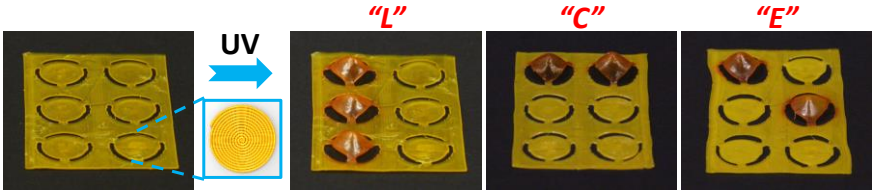

Shape-switching liquid crystal elastomers are formulated where light is used to trigger a shape change which is then stable indefinitely. The original shape can be recovered on heating. These materials can be 4D printed into reconfigurable Braille-like actuators capable of displaying letters "L", "C" and "E" by switching the shape-morphing of the Archimedean chord patterns with UV light and heating.